Mutant SOD1 in cell types other than motor neurons and oligodendrocytes accelerates onset of disease in ALS mice

Koji Yamanaka*[†], Severine Boillee*, Elizabeth A. Roberts[‡], Michael L. Garcia*[§], Melissa McAlonis-Downes*, Oliver R. Mikse*, Don W. Cleveland*[¶], and Lawrence S. B. Goldstein[‡¶]

*Ludwig Institute for Cancer Research and Department of Medicine and Neuroscience, University of California at San Diego, La Jolla, CA 92093; [†]Yamanaka Research Unit, RIKEN Brain Science Institute, Wako, Saitama 351-0198, Japan; [‡]Howard Hughes Medical Institute and Department of Cellular and Molecular Medicine, School of Medicine, University of California at San Diego, La Jolla, CA 92093; and [§]University of Missouri, Columbia, MO 65211

Contributed by Don W. Cleveland, March 13, 2008 (sent for review January 26, 2008)

Dominant mutations in ubiquitously expressed superoxide dismutase (SOD1) cause familial ALS by provoking premature death of adult motor neurons. To test whether mutant damage to cell types beyond motor neurons is required for the onset of motor neuron disease, we generated chimeric mice in which all motor neurons and oligodendrocytes expressed mutant SOD1 at a level sufficient to cause fatal, early-onset motor neuron disease when expressed ubiquitously, but did so in a cellular environment containing variable numbers of non-mutant, non-motor neurons. Despite high-level mutant expression within 100% of motor neurons and oligodendrocytes, in most of these chimeras, the presence of WT non-motor neurons substantially delayed onset of motor neuron degeneration, increasing disease-free life by 50%. Disease onset is therefore non-cell autonomous, and mutant SOD1 damage within cell types other than motor neurons and oligodendrocytes is a central contributor to initiation of motor neuron degeneration.

cell autonomous | motor neuron disease

Amyotrophic lateral sclerosis (ALS) is an adult-onset neurodegenerative disease characterized by the selective loss of motor neurons, which results in progressive and ultimately fatal paralysis of skeletal muscles leading to death usually within 2 to 5 years after disease onset. Ten percent of cases of ALS are inherited, and the most frequent causes of familial ALS are dominant mutations in the gene for Cu/Zn superoxide dismutase (SOD1). Whereas deletion of SOD1 from mice does not cause motor neuron disease, ubiquitous expression of mutant SOD1 in rodents leads to progressive, selective motor neuron degeneration, arising from an acquired toxicity of mutant SOD1. Although several hypotheses have been proposed to explain the mechanism of mutant SOD1-mediated toxicity (including formation of protein aggregates because of reduced conformational stability, mitochondrial dysfunction, excitotoxicity, abnormal axonal transport, mutant-derived oxidative damage, lack of growth factors, and inflammation), the exact mechanisms responsible for the onset, and then the progression, of motor neuron degeneration remain unknown (1–3).

A central unsolved question is how the surrounding environment affects mutant SOD1-expressing motor neurons. Whereas initial efforts to selectively express mutant SOD1 in neurons (4, 5) failed to cause motor neuron degeneration or disease, pan-neuronal mutant expression (from the Thy1 promoter) did yield very late onset disease in one mouse line, but even that disease progressed very slowly (6). Construction and analysis of chimeric mice initially implicated cells neighboring motor neurons as important players in determining survival (7). Subsequently, we and others demonstrated that selective reduction in mutant SOD1 expression within microglia (8, 9) and astrocytes (10) significantly slows the progression of disease, but, surprisingly, does not affect the timing of disease onset. Among several possibilities, acceleration of progression by mutant astrocytes could depend on glutamate-dependent excitotoxicity due to loss of the EAAT2 glutamate transporter from affected regions (11), an enhanced inflammatory response from microglia mediated by mutant-expressing astrocytes (10), inability to regulate glutamate receptor subunit 2 (GluR2) expression in motor neurons by mutant astrocytes (12), or release by astrocytes of one or more unknown toxic factors, as suggested by accelerated death *in vitro* of embryonic stem cell-derived motor neurons when cocultured with mutant expressing glial cells or conditioned media from those cells (13, 14). Together, these data raised the possibility that accelerated disease progression does not alter the timing of disease onset.

Evidence that disease onset might have different genetic and cellular determinants than disease progression comes from the recent demonstration that selective down-regulation of mutant SOD1 solely within the postnatal motor neurons (for example, using vesicular acetylcholine transporter promoter-driven Cre mice (15) and a deletable "floxed" mutant SOD1 transgene) significantly slowed onset without affecting disease progression (10). Recent work also demonstrated that pan-neuronal expression of mutant SOD1 in mice (using the Thy-1 promoter) resulted in very late onset motor neuron disease (6). However, unresolved is whether onset of disease from this neuron-specific mutant synthesis is delayed when compared with mice expressing mutant SOD1 at comparable levels within motor neurons and also expressing the mutant ubiquitously.

It therefore remains untested whether the onset of mutant SOD1-mediated ALS is determined solely by cell-autonomous mechanisms. Whereas mutant microglia and astrocytes strongly accelerate disease progression (8–10), and mutant synthesis selectively within astrocytes can yield astrocytic activation, but not motor neuron degeneration (16), the influence of mutant expression within cell types beyond motor neurons on the onset of degeneration is unknown. To resolve these issues, we created aggregation chimeras derived from embryonic cells of $SOD1^{G37R}$ mice (17) and embryonic cells from mice lacking the Olig1 and Olig2 transcription factors ($Olig^{-/-}$) (18) to analyze disease in mice in which all motor neurons (and oligodendrocytes) express high levels of mutant SOD1.

Results

$Olig^{-/-}$::$SOD1^{G37R}$ Chimeric Mice. Our goal was to generate mice in which all motor neurons were derived solely from an $SOD1^{G37R}$ mutant mouse line that develops early-onset disease (17) but in

Author contributions: K.Y., S.B., and E.A.R. contributed equally to this work; K.Y., S.B., E.A.R., D.W.C., and L.S.B.G. designed research; K.Y., S.B., E.A.R., M.L.G., M.M.-D., and O.R.M. performed research; K.Y., S.B., E.A.R., M.L.G., M.M.-D., D.W.C., and L.S.B.G. analyzed data; and K.Y., S.B., D.W.C., and L.S.B.G. wrote the paper.

The authors declare no conflict of interest.

[¶]To whom correspondence may be addressed. E-mail: dcleveland@uscd.edu or lgoldstein@ucsd.edu.

This article contains supporting information online at www.pnas.org/cgi/content/full/0802556105/DCSupplemental.

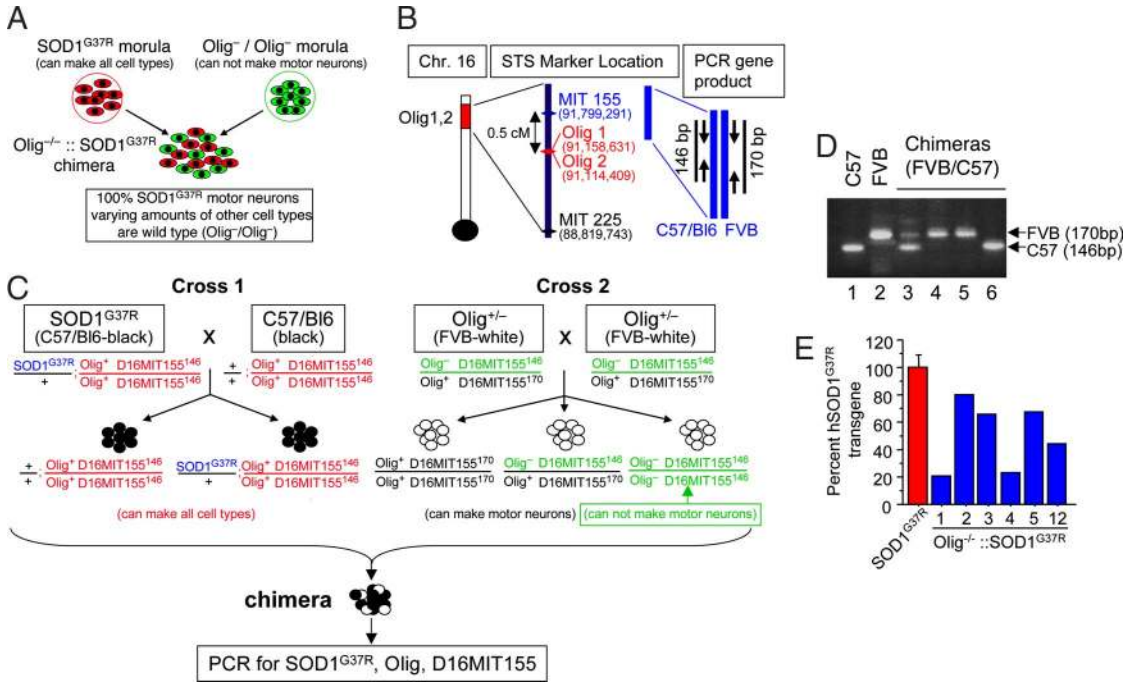

Fig. 1. Strategy for generating Olig$^{-/-}$::SOD1^{G37R} chimeric mice. (*A*) Experimental design for creation of chimeric mice that have 100% SOD1^{G37R} motor neurons. (*B*) Location of the Olig1/2 locus and D16MIT155 STS marker on mouse chromosome 16. (*C*) Mating and genotyping strategy for generating Olig$^{-/-}$::SOD1^{G37R} chimeric mice. Olig$^{+/-}$ mice used for Cross 2 were generated by the mating of Olig$^{+/-}$ mice (C57BL/6 genetic background) with WT FVB mice. The SOD1^{G37R} mice were of a C57BL/6 genetic background (the WT Olig^{+} allele from SOD1^{G37R} mice is highlighted in red). Expected genotypes of each embryo are described. Olig$^{-/-}$ embryos were generated by intercrossing Olig$^{+/-}$ mice (Cross 2). Chimeras derived from Olig$^{-/-}$ embryos were distinguished from Olig$^{+/-}$ by using the D16MIT155 STS marker, which is closely located near the Olig1/2 locus. The Olig^{-} allele derived from the C57BL/6 background carries MIT155^{146} (highlighted in green). (*D*) PCR products of the D16MIT155 STS marker. A PCR product of 146 bases is produced from the C57BL/6 background or Olig$^{-/-}$::SOD1^{G37R} or Olig$^{-/-}$::WT chimeras (lanes 1 and 6), whereas chromosome 16 derived from FVB mice produces a PCR product of 170 base (D16MIT155^{170}, lanes, 2, 4, and 5). (*E*) Degree of chimerism of Olig$^{-/-}$::SOD1^{G37R} mice assessed by Q-PCR for the SOD1^{G37R} transgene. Duplex Q-PCR (three independent runs) on genomic DNA from tail extracts was used to analyze the levels of SOD1 mutant transgene. Tail DNA extracts from the original SOD1^{G37R} line 42 (n = 2) were used as positive controls and assigned a 100% transgene content (red bar).

which other cell types would have varying proportions of mutant and normal cells. Such chimeric mice were produced by aggregation of cells from morula stage SOD1^{G37R} embryos (which can generate all cell types) and embryos deficient in the Olig1 and Olig2 (Olig$^{-/-}$) transcription factors; these homozygous mutants are unable to generate motor neurons and oligodendrocytes and ordinarily die before birth (Fig. 1*A*).

To distinguish chimeric mice derived from Olig$^{+/-}$ and Olig$^{-/-}$ mice, we used differential marking of the Olig^{+} allele. Thus, Olig$^{-/-}$ embryos were generated by intercrossing of Olig$^{+/-}$ mice in which the Olig^{+} allele was marked with a sequence length polymorphism found in the FVB mouse strain (a 24-base insertion) at the D16MIT155 locus (Gene ID: 62773, UniSTS:127788) that lies 0.5 cM from the Olig gene (Fig. 1*B*). The tight linkage between D16MIT155 and the Olig genes was confirmed by the observed lack of recombination among 113 offspring obtained from the breeding of Olig$^{+/-}$ mice (D16MIT155$^{170/146}$). Thus, all chimeras derived from either WT or heterozygous Olig embryos would generate a 170-bp fragment (D16MIT155^{170}) after PCR of tail genomic DNA (Fig. 1 *B* and D and supporting information (SI) Fig. S1). However, the absence of the expanded D16MIT155 allele in similar PCRs of genomic DNA from each chimera would be diagnostic for chimeras derived from Olig$^{-/-}$ embryos (Fig. 1 *B* and D, lane 6). Subsequently immunocytochemistry was used to confirm that all motor axons in these Olig$^{-/-}$ chimeras were in fact mutant (see Fig. 2*A*).

Although no Olig1/2-deficient or Olig2-deficient mice are viable postnatally because of the absence of motor neurons (18–20), 25 of 100 viable chimeras (as judged by mottled coat color) contained Olig$^{-/-}$ cells (Fig. 1*C* and Fig. S1). Approximately half of these Olig$^{-/-}$ chimeras showed abnormal limb posture, which was evident early in life (Table 1). In most cases, one or two limbs (either forelimbs or hindlimbs) were contracted (Movies S1 and S2). Because these abnormalities of limb posture and ambulatory activity were not progressive and were of comparable severity and frequency in Olig$^{-/-}$ chimeras fused with either WT or SOD1^{G37R} mutant embryos, they cannot result from SOD1 mutant derived damage. Instead, they must reflect congenital abnormalities probably resulting from one or more developmental deficits associated with lack of proper Olig function, i.e., Olig$^{-/-}$.

Seven chimeras derived from an SOD1^{G37R}-positive embryo and an Olig$^{-/-}$ embryo were identified by the presence of the SOD1^{G37R} transgene and homozygosity at the marked Olig$^{-/-}$ locus (D16MIT155$^{146/146}$) (Fig. S1). These Olig$^{-/-}$::SOD1^{G37R} chimeras were found at approximately the expected frequency and with varying degrees of chimerism, as measured either by coat color or by proportion of SOD1^{G37R} transgenes within genomic tail DNA (Fig. 1*E*).

All Motor Neurons in Olig$^{-/-}$::SOD1^{G37R} Chimeras Are Mutant SOD1-Expressing. To test whether all motor neurons of Olig$^{-/-}$::SOD1^{G37R} chimeras expressed mutant SOD1 as expected from the prior genetic efforts, the fifth lumbar (L5) ventral and dorsal roots were immunostained with human-specific SOD1 antibody. Transverse sections of L5 ventral roots showed that all motor axons of Olig$^{-/-}$::SOD1^{G37R} chimeras expressed human SOD1^{G37R} (Fig. 2 *A* and *B*), yielding images (and fluorescence intensities) comparable with the analysis of germ-line SOD1^{G37R} roots (Fig. 2*D*). Lumbar spinal cord sections from different levels were stained with human SOD1 antibody and SMI-32, a marker for neurons. All motor neurons examined from different levels of lumbar spinal cord expressed human SOD1 (Fig. 2 *F–K*), confirming that

Table 1. Characteristics of Olig$^{-/-}$::SOD1^{G37R} and Olig$^{-/-}$::WT chimeric mice

ID	SOD1^{G37R}	Survival, days	Disease	Abnormal limb posture at birth	L4 motor axon (R/L)	L5 motor axon (R/L)
1	+	239	No	Yes	271/326	454/407
2	+	234	No	No	403/549	595/680
3	+	224	No	Yes	341/488	410/ND
4	+	211	No	Yes	405/284	543/314
5	+	192	Yes	Yes	544/ND	757/746
6	−	395	No	No	477/541	511/886
7	−	368	No	No	463/473	839/743
8	−	366	No	Yes	ND/241	323/456
9	−	269	No	Yes	584/457	ND/517
10	−	269	No	No	612/399	664/606
11	−	267	No	No	845/760	873/908
12	+	65	No	No	573/486	492/397
13	−	65	No	Yes	438/301	418/435
Mean Olig$^{-/-}$:: SOD1^{G37R}					424 ± 109 (n = 11)	526 ± 150 (n = 11)
Mean Olig$^{-/-}$:: WT					507 ± 166 (n = 13)	629 ± 202 (n = 13)

Survival ages of SOD1^{G37R} positive chimeras (ID nos. 1–5 and 12) and control chimeras (nos. 6–11 and 13). All chimeras but chimera no.5 were killed for the histological analysis before showing hindlimb paralysis or other disease. ND, not determined.

Olig$^{-/-}$::SOD1^{G37R} chimeras had 100% mutant SOD1-expressing motor neurons. In contrast, the dorsal roots of Olig$^{-/-}$::SOD1^{G37R} chimeras showed only a proportion of human SOD1-positive axons, indicating that sensory axons were chimeric for WT and mutant SOD1-expressing axons (Fig. 2*C*).

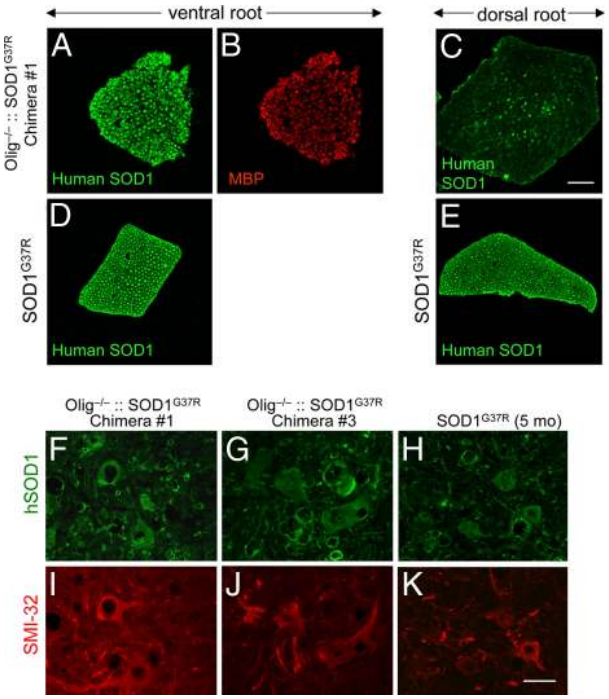

Fig. 2. Olig$^{-/-}$::SOD1^{G37R} chimeric mice express mutant SOD1 in all motor neurons but only in a subset of sensory axons. (*A–E*) L5 ventral (motor), (*A*, *B*, and *D*) and dorsal (sensory) (*C* and *E*) roots from 8-month-old Olig$^{-/-}$::SOD1^{G37R} mice (*A–C*) or 2-month-old germ-line SOD1^{G37R} mice (*D* and *E*) were stained with human specific SOD1 antibody (*A* and *C–E*), or myelin basic protein antibody (*B*). (*F–K*) Lumbar spinal cord sections from two different Olig$^{-/-}$::SOD1^{G37R} and 5-month-old SOD1^{G37R} mice immunostained with the anti-human SOD1 antibody (*F–H*) and the motor neuron marker SMI-32 (*I–K*). Note that all of the motor neurons are SMI-32-positive (red) and also expressed human SOD1 (green). [Scale bars: 50 μm (*A–E*) and 40 μm (*F–K*).]

Variable, Olig$^{-/-}$-Mediated Reduction in Motor Neuron Number in WT or SOD1^{G37R} Chimeras. Examination of transverse sections (Fig. 3 *A–G* and Fig. S2) of motor roots (stained with toluidine-blue) revealed that the number of both L5 and L4 motor axons of the Olig$^{-/-}$ chimeras had unexpected variability relative to those found in germ-line normal or SOD1^{G37R} mice. The reduced number of motor axons (frequently also highly asymmetric in comparing right and left roots; Table 1) was not, however, the result of mutant SOD1-dependent axonal loss. Similarly reduced numbers and variability of motor axons were seen in Olig$^{-/-}$::WT chimeras and Olig$^{-/-}$::SOD1^{G37R} chimeras. The reduced axonal number was in some cases extraordinary: instead of the typical ≈1,000 axons in the L5 root, some WT and SOD1^{G37R} chimeras had roots with as few as 323 and 314 motor axons in Olig$^{-/-}$::WT and Olig$^{-/-}$::SOD1^{G37R} chimeras, respectively. There was no statistically significant difference in number of motor axons from Olig$^{-/-}$::SOD1^{G37R} and Olig$^{-/-}$::WT (mean axon number ± standard error for L4, SOD1^{G37R}, 424 ± 109; WT, 507 ± 106, $P = 0.17$; for L5, SOD1^{G37R}, 526 ± 150; WT, 629 ± 202, $P = 0.18$, unpaired t test) (Table 1). Because reduced axon numbers were found early in life and did not seem to increase with age (Table 1; Fig. 3*E*), and because there was an absence of signs of significant active axonal degeneration (Fig. 3*F* and Fig. S2), the variable number of motor axons almost certainly reflects loss of motor neurons early in development that normally would have been contributed by Olig$^{-/-}$ progenitor cells.

Motor neuron disease from expression of mutant SOD1 has previously been demonstrated to arise from loss of the pool of large caliber motor axons (21), including for end-stage mutant SOD1^{G37R} (22) (see also Fig. 3 *A* and *E*). With the exception of one Olig$^{-/-}$::SOD1^{G37R} chimera (no. 5, Table 1, Fig. 3*D*) that developed ALS-like hindlimb weakness, the Olig$^{-/-}$::SOD1^{G37R} chimeras (nos. 1–4, 7–8 months old), however, did not have a reduced proportion of the large (>3 μm in diameter) axons when compared with WT mice (Fig. 3 *A*, C, and E), reflecting preservation of large caliber motor axons of Olig$^{-/-}$::SOD1^{G37R} chimeras (Fig. 3*F*). Further, examination of transverse sections of spinal cords from

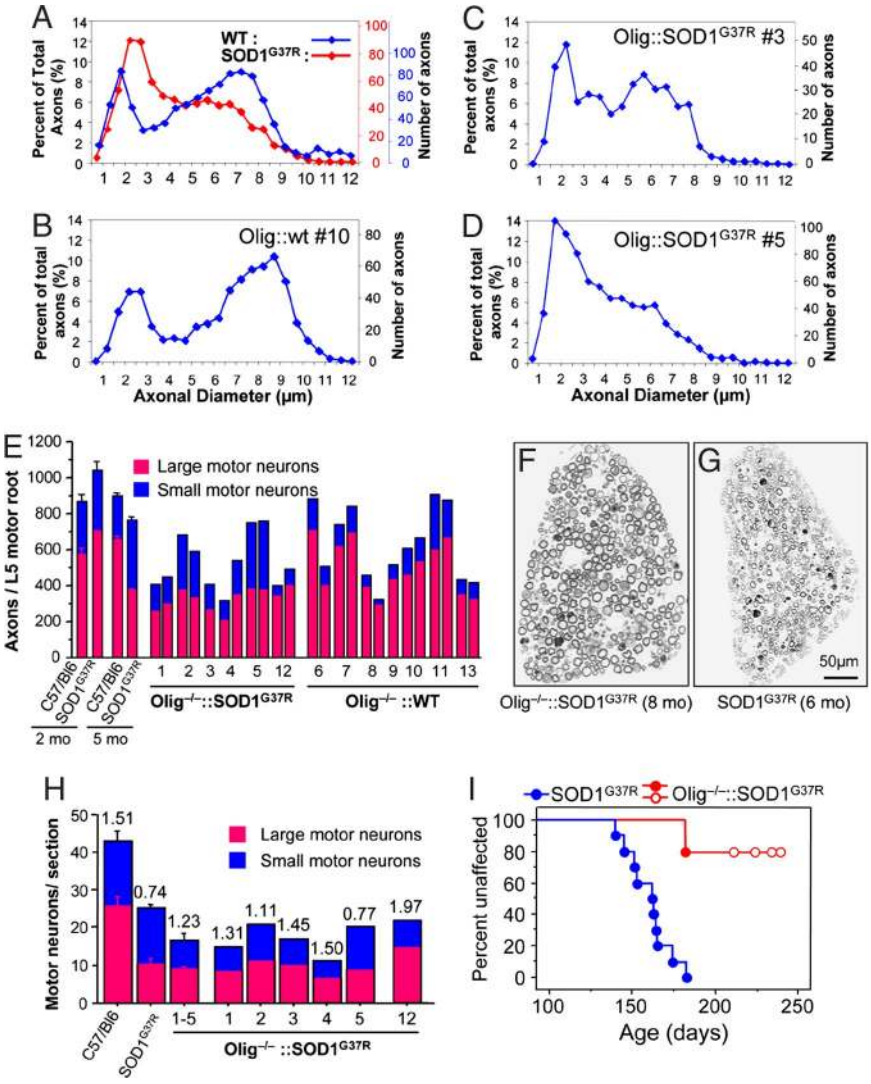

Fig. 3. Mutant SOD1-expressing motor neurons of Olig$^{-/-}$::SOD1^{G37R} escaped degeneration. (*A–D*) Representative L5 motor axonal caliber of WT (*A*, blue), end-stage SOD1^{G37R} (*A*, red), Olig$^{-/-}$::WT chimera (*B*), and Olig$^{-/-}$::SOD1^{G37R} chimeras (*C* and *D*). (*B–D*) Averaged axon caliber counts of both side of L5 motor roots (an average of three to four animals per genotype in *A*). (*D*) Note only no. 5 chimera developed ALS-like disease. (*E*) The number and proportions of large (>3-μm diameter, red bars) and small caliber motor axons (blue bars) in the L5 motor roots from various chimeras (numbers corresponding to the ID in Table 1), germ-line SOD1^{G37R}, and C57BL/6 mice. For the number of axons in SOD1^{G37R} and C57BL/6 mice, an average from three to four animals per genotype was shown. (*F* and *G*) Representative toluidine-blue-stained L5 motor axon images of 8-month-old Olig$^{-/-}$::SOD1^{G37R} mice (*F*), and end-stage SOD1^{G37R} mice (6 months old, *G*). (*H*) Quantification of large motor neurons (red bars) and small motor neurons (blue bars); sample images are in Fig. S3). Bars represent the mean number of motor neurons per section averaged from 10–12 sections cut throughout the lumbar spinal cords. The numbers on top of the bars represent the ratio of the number of large motor neurons to the number of small motor neurons. [Scale bar: 50 μm (*F* and *G*).] (*I*) Olig$^{-/-}$::SOD1^{G37R} chimeric mice are viable and escaped from motor neuron disease. Shown are onset data of germ-line SOD1^{G37R} mice (blue) and Olig$^{-/-}$::SOD1^{G37R} chimeric mice (red). Open circles indicate four chimeric mice that never developed motor neuron disease but that were killed at 211–239 days of age.

Olig$^{-/-}$::SOD1^{G37R} chimeras confirmed that large motor neurons, which were mainly lost in the end-stage SOD1^{G37R} mice (Fig. S3*B*), were preserved in the Olig$^{-/-}$::SOD1^{G37R} chimeras (Fig. S3 *C* and *D*). The ratio of large to small motor neurons in most Olig$^{-/-}$::SOD1^{G37R} chimeras (nos. 1–4) was comparable with that in normal mice, but not to the reduced ratio measured in end-stage SOD1^{G37R} mice (Fig. 3*H*). Combined with the absence of active degeneration within the motor roots, we conclude that, although all motor neurons were mutant and some chimeras (e.g., nos. 1 and 3) had the substantial disadvantage of as few as one-third the normal number of motor neurons surviving during development, there was little, if any, mutant-dependent motor neuron loss in the Olig$^{-/-}$::SOD1^{G37R} chimeras at ages 28 (chimera no. 4) to 56 (chimera no. 1) days past the 183 days of maximal age of disease onset of the germ-line SOD1^{G37R} mice. Finally, examination of spinal cord sections of these disease-free chimeric mice for hallmark cellular signs of disease revealed an absence of ubiquitinated protein accumulation in SOD1 mutant motor neurons, and a comparatively modest level of astrocytic and microglial activation relative to end-stage germ-line SOD1^{G37R} mice, and relative to chimeric mouse no. 5, which developed disease (Figs. S4 and S5).

Most Olig$^{-/-}$::SOD1^{G37R} Chimeras Escape Early-Onset Motor Neuron Disease. Of seven Olig$^{-/-}$::SOD1^{G37R} chimeras that were carefully monitored during aging, one died suddenly from an unknown cause at 151 days of age, but without prior motor neuron symptoms. One (chimera no. 12) was killed at 65 days of age for histological experiments. For the remaining five, one chimera (no. 5, Table 1) was killed at 192 days of age, after it developed partial hindlimb paralysis, a symptom indicating initiation of motor neuron disease. The remaining four chimeras, killed at ages between 211 and 239 days (Fig. 3*I*, open circles), all continued to move without difficulty and could reach food and water without any assistance despite some limb abnormalities present as early as weaning age. None, however, developed any phenotypic signs of age-dependent motor neuron disease (Movies S3 and S4) by an age of 51–79 days beyond the mean onset of germ-line SOD1^{G37R} mice (160 days of age, Fig. 3*I*), indicating as much as a 1.5-fold increase of disease-free life achieved in those chimeras. These disease-free mice also did not exhibit the weight loss that typically accompanies phenotypic disease onset. Thus, these animals exhibited no signs of the onset of ALS despite having all of their motor neurons mutant for SOD1.

Mutant Upper Motor Neurons Escape Age-Dependent Degeneration in Olig$^{-/-}$::SOD1^{G37R} Chimeras. In symptomatic mutant SOD1 mice, spinal lateral axons, which contain axons of the upper motor neurons, are severely degenerated (23). To examine whether the WT non-motor neuronal cells affect degeneration of these upper motor axons, morphology of spinal lateral axons in the lumbar spinal cords was examined in the Olig$^{-/-}$::SOD1^{G37R} chimeras.

NEUROSCIENCE

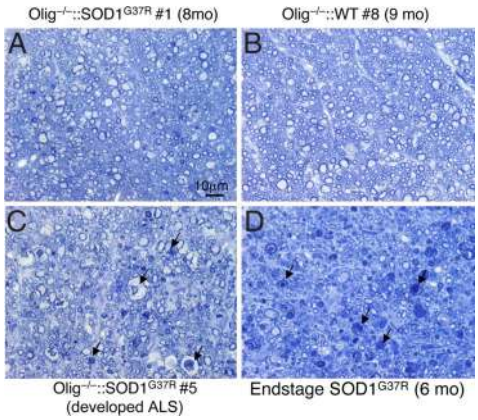

Fig. 4. Upper motor axons in the lateral spinal cord are preserved in Olig$^{-/-}$::SOD1^{G37R} mice. Transverse sections of upper lumbar spinal cord of Olig$^{-/-}$::SOD1^{G37R} chimera no. 1 (*A*), Olig$^{-/-}$::WT (*B*), Olig$^{-/-}$::SOD1^{G37R} chimera no. 5 (*C*, developed ALS), or end-stage SOD1^{G37R} mice (*D*) were stained with toluidine blue. Arrows, degenerating axons. (Scale bar: 10 μm.)

Parallel analysis of end-stage SOD1^{G37R} mice (6 months old) showed severe degeneration in the spinal lateral axons as expected (Fig. 4*D*), as well as in the one Olig$^{-/-}$::SOD1^{G37R} chimera (no. 5, Fig. 4*C*) that developed motor neuron disease at 192 days of age. In contrast, despite all motor neurons and their ensheathing oligodendrocytes expressing mutant SOD1, almost all lateral axons of the remaining Olig$^{-/-}$::SOD1^{G37R} chimeras including the one killed at the oldest age (8 months) (Fig. 4*A*) were preserved (just as they were in Olig$^{-/-}$::WT chimeras (Fig. 4*B*)).

Discussion

Despite the fact that all motor neurons of the Olig$^{-/-}$::SOD1^{G37R} mice expressed the SOD1^{G37R} transgene at a level comparable with that in germ-line SOD1 mutant mice that develop early-onset motor neuron disease when expressed ubiquitously, four of five Olig$^{-/-}$::SOD1^{G37R} chimeras escaped any sign of onset of motor neuron disease without showing overt motor neuron degeneration for as much as 53 days beyond the mean life span of germ-line SOD1^{G37R} mice. Evidence that the expression level of mutant SOD1 in motor neurons of Olig$^{-/-}$::SOD1^{G37R} mice was comparable with that in germ-line SOD1^{G37R} mice comes from the one chimera (no. 5) that developed motor neuron disease, probably because of a large contribution of mutant-expressing cells other than motor neurons. In fact, and to our surprise, a highly significant, 1.5-fold, increase in disease-free life was documented in these surviving animals before killing for experimental analysis. Preservation of upper and lower motor neurons in these chimeras clearly indicated that expression of mutant SOD1 in all motor neurons was not sufficient to cause onset and hence progression of early-onset disease or motor neuron degeneration. Thus, although the number of Olig$^{-/-}$::SOD1^{G37R} chimeric mice produced for this study was relatively small because of the complexity of the experimental design, our data establish that onset of motor neuron degeneration is non-cell autonomous and that non-autonomous cell contributors to onset may be distinguishable from those that drive progression because accelerating disease progression [from reduced mutant synthesis in astrocytes (10) or microglia (9)] was not previously observed to affect the timing of disease onset.

We note that Olig$^{-/-}$ chimeras had fewer motor neurons as early as 65 days of age independent of the expression of the SOD1^{G37R} transgene. Although there was variation in the number of L4 and L5 motor axons (ranging from 241 to 845 axons in L4, 314–908 axons in L5), the average number of motor axons of Olig$^{-/-}$ chimeras was approximately half that of WT mice. This finding is also striking because these chimeric mice escaped phenotypic signs of motor neuron disease onset despite a comparative disadvantage beginning early in life, i.e., having substantially fewer motor neurons than normal, which might have been expected to sensitize these animals to motor neuron damage. Whereas prior lesioning of motor axons using peripheral axotomy has been reported to increase the proportion of small caliber axons and reduce motor neuron vulnerability to mutant SOD1 (24), our Olig$^{-/-}$::SOD1^{G37R} mice retain a high proportion of the large caliber motor axons that are vulnerable to motor neuron disease. Nevertheless, these large-caliber mutant-containing motor axons escaped degeneration.

Selective gene inactivation within motor neurons has proven that the timing of disease onset can be delayed by reducing mutant SOD1 solely within postnatal motor neurons (10). Whereas no work to date had provided any insight into whether damage to cell types beyond motor neurons was a determinant of disease onset, our chimeras now establish that mutant SOD1 action within one or more additional cell types affects timing of disease onset. Indeed, in addition to escape from disease onset in most Olig$^{-/-}$::SOD1^{G37R} mice, only a small subset of mutant-expressing motor axons exhibited any degenerative changes. Even then, the degree of degeneration never reached the level that was required to support motor neuron disease.

As to the identity of the cell types beyond motor neurons that contribute to disease onset, mutant synthesis within muscle has previously been shown not to affect either onset or progression (25). Mutant synthesis within microglia (8, 9) or astrocytes (10) strongly accelerates disease progression, but expression in neither cell type seems to affect onset. The inability to generate oligodendrocytes in Olig1/2$^{-/-}$ mice (18) predicts that Olig$^{-/-}$::SOD1^{G37R} mice express mutant SOD1 in all oligodendrocytes as well as motor neurons (technical limitations precluded documenting that all oligodendrocytes were mutant). If so, then mutant SOD1 expression by oligodendrocytes is also not a significant contributor to degeneration of upper motor neurons and disease onset. Although it remains untested whether mutant toxicity solely within motor neurons is sufficient to provoke motor neuron disease, pan-neuronal expression of mutant SOD1 in mice was recently shown to result in very late onset motor neuron disease (6), suggesting that neurons other than motor neurons are contributors to onset of disease. Potential contributors to disease onset remain untested, but include mutant SOD1 action within interneurons, the myelinating Schwann cells of the periphery, and the endothelial cells of the vasculature. Consistent with damage directly developed within the last of these cell types, SOD1 mutants of different biochemical characteristics disrupt the blood–spinal cord barrier by reducing the levels of the tight junction proteins ZO-1, occludin and claudin-5, resulting in microhemorrhages with release of neurotoxic hemoglobin-derived products, reductions in microcirculation, and hypoperfusion. SOD1-mutant mediated endothelial damage accumulates before motor neuron loss and a neurovascular inflammatory response (26), supporting a central contribution to disease initiation.

In any event, the cumulative evidence supports the hypothesis that it is ALS-linked mutant SOD1 within multiple cell types that, in collaboration with damage directly within motor neurons, drives non-cell-autonomous onset of motor neurodegeneration.

Materials and Methods

Generation of Chimeric Mice. Olig$^{-/-}$::SOD1^{G37R} chimeric mice were generated by aggregation of embryos (morulae at eight-cell stage) derived from Olig$^{+/-}$ × Olig$^{+/-}$ and from SOD1^{G37R} $^{+/-}$ (line 42) × C57BL/6 breedings (17). Olig$^{+/-}$ mice were generated by the breeding of FVB mice and Olig1/2 mutant heterozygous mice (a gift from D Anderson, California Institute of Technology) (18).

Mice were genotyped by PCR for the presence of the mutant SOD1 transgene as described in ref. 27, and for the Olig mutant locus using the following primers: sense, GAA CAG CAG CAG CAG CAG CTG; antisense, CAG CTC CTG CG CGA GCT ACC.

To distinguish chimeras derived from Olig$^{-/-}$ embryos from those from Olig$^{+/-}$ embryos, a Sequence-Tagged-Site (STS) marker D16MIT155 located 0.7 Mb telomeric from the Olig1/2 locus was used. We exploited the situation that in our

matings the Olig WT locus we used was derived from FVB mice, whereas the Olig mutant locus was derived from a C57BL/6 allele. This situation yielded a 170-bp PCR product (D16MIT155^{170}) for the STS locus in any animal with one unmutated Olig allele (see Fig. 1 *B* and *D*), but only a 146-bp product (D16MIT155^{146}) for chimeras generated from mutant SOD1 embryos and embryos homozygously deleted for Olig. The primers used for D16MIT155 were the following: primer 1, AAA CAC AAG GTT ATC TTA GTG GTG G; primer 2, TGT GTT TGT ATA TGT GAA TGT ATG TCA.

For survival experiments, the time of onset was defined at the time when denervation-induced muscle atrophy had produced a 10% loss of maximal body weight, and end-stage was determined by paralysis sufficiently severe that the animal could not right itself within 20 seconds when placed on its side, an endpoint frequently used for SOD1 mutant-expressing mice (e.g., refs. 9 and 28) and one that was consistent with the requirements of the Animal Care and Use Committee of the University of California. Animals were observed every 24 h.

Quantification of SOD1 Transgene Level by Real-Time PCR. To estimate the overall degree of chimerism, genomic DNA extracted from tails was analyzed by quantitative PCR of the human SOD1 gene as described in ref. 9. In brief, DNA (33 ng) was amplified with iQ supermix (Bio-Rad) and 100 nM of each primer and probe in a Bio-Rad iCycler real time PCR machine. The specific primers and probe used for the human SOD1 gene were the following: hSOD1-forward, CAATGTGACTGCTGACAAAG; hSOD1-reverse, GTGCGGC-CAATGATGCAAT; and hSOD1 probe, fam-CCGATGTGTCTATTGAAGATTCTG-BHQ. Primers and probe for the apolipoprotein B (apoB) as a normalizer were as follows: apoB-forward, CACGTGGGCTCCAGCATT; apoB-reverse, TCAC-CAGTCATTTCTGCCTTTG; and apoB probe, Texas Red-CCAATGGTCGGG-CACTGCTCAA-BHQ2.

Tissue Preparation and Immunofluorescence. Mice were perfused transcardially with PBS followed by 4% paraformaldehyde in phosphate buffer. Before freezing, tissues were cryoprotected in 30% (wt/vol) sucrose in PBS. Frozen tissues were sectioned with a cryostat (Leica, Bannockburn, IL) in 30-μm or 20-μm sections for spinal cord or roots, respectively, and processed for immunofluorescence.

Floating sections of spinal cords were incubated in blocking buffer [1% (wt/vol) BSA, 0.2% (wt/vol) fat-free milk, 5% (vol/vol) normal goat serum, 0.3% (vol/vol) Triton X-100 in PBS, pH 7.4], followed by overnight incubation with a set of two primary antibodies; an antibody recognizing unphosphorylated neurofilaments, SMI32 (1:1000, Sternberger Monoclonals, Lutherville MA) and hSOD1 (1:100) (7, 29) diluted in PBS/0.3% Triton X-100 (PBST). Subsequently, the sections were incubated with species-specific secondary antibodies that were conjugated with either FITC or Cy3 (Jackson ImmunoResearch, West Grove, PA).

For the staining of roots, sections were directly mounted on slides and incubated in blocking buffer [1% (wt/vol) BSA, 1% (vol/vol) goat serum, 0.3% (vol/vol) Triton X-100 in PBS, pH 7.4], followed by incubation with hSOD1 antibody (diluted at 1:300) and myelin basic protein (MBP) antibody (1:100, Chemicon) in PBST overnight and subsequently with anti-rabbit and anti-rat IgG antibodies that were conjugated with FITC and Texas Red (Jackson ImmunoResearch, West Grove, PA), respectively. Sections were mounted in ProLong Antifade reagent (Invitrogen, Carlsbad, CA) and analyzed on an Olympus confocal microscope (FV1000).

Immunohistochemistry and Evaluation of Microgliosis and Astrogliosis. Floating sections of spinal cords were incubated with primary antibodies followed by biotinylated species-specific secondary antibodies. Details are provided in *SI Materials and Methods*.

Motor Neuron Counting. Motor neuron numbers were determined from 30-μm-serial sections across the lumbar spinal cords (a total of 10–12 sections per animal). Motor axons were counted in every 24th section after staining with anti-ChAT antibody.

Morphological Analysis of Axons. Spinal cords and lumbar roots, postfixed in 4% paraformaldehyde/PBS, transversely sectioned into 5-mm blocks were treated with 2% Osmium tetroxide in 0.05 M cacodylate buffer, washed, dehydrated, and embedded with Epon (Electron Microscopy Sciences). One-micrometer cross-sections were stained with 1% toluidine blue. Axonal diameters of L5 or L4 roots were measured by Bioquant software. Entire roots were imaged, imaging thresholds were selected individually, and the cross-sectional area of each axon was calculated and reported as a diameter of a circle of equivalent area. Axon diameters were grouped into 0.5-μm bins.

ACKNOWLEDGMENTS. All fluorescent microscopy acquisitions were done at the University of California at San Diego Neuroscience Microscopy Shared Facility (National Institute of Neurological Diseases and Stroke P30 NSO47101). This work was supported by National Institutes of Health Grant NS 27036 (to D.W.C.) and by the Packard ALS Center at The Johns Hopkins University (D.W.C. and L.S.B.G.). Salary support for D.W.C is provided by the Ludwig Institute for Cancer Research. L.S.B.G. is an Investigator of the Howard Hughes Medical Institute. K.Y. was supported by a Career Development grant from the Muscular Dystrophy Association (MDA), the Uehara Memorial Foundation, the Nakabayashi Trust for ALS Research, and Grants-in-aid for Scientific Research (Grants 19591021 and 19044048) from the Ministry of Education, Culture, Sports, Science and Technology of Japan. S.B. was supported, in part, by a Fondation pour la Recherche Medical fellowship, an Institut National de la Santé et de la Recherche Médicale fellowship, and a Career Development grant from the MDA.

1. Bruijn LI, Miller TM, Cleveland DW (2004) Unraveling the mechanisms involved in motor neuron degeneration in ALS. *Annu Rev Neurosci* 27:723–749.
2. Boillee S, Vande Velde C, Cleveland DW (2006) ALS: A disease of motor neurons and their nonneuronal neighbors. *Neuron* 52:39–59.
3. Pasinelli P, Brown RH (2006) Molecular biology of amyotrophic lateral sclerosis: Insights from genetics. *Nat Rev Neurosci* 7:710–723.
4. Pramatarova A, *et al.* (2001) Neuron-specific expression of mutant superoxide dismutase 1 in transgenic mice does not lead to motor impairment. *J Neurosci* 21:3369–3374.
5. Lino MM, Schneider C, Caroni P (2002) Accumulation of SOD1 mutants in postnatal motoneurons does not cause motoneuron pathology or motoneuron disease. *J Neurosci* 22:4825–4832.
6. Jaarsma D, *et al.* (2008) Neuron-specific expression of mutant superoxide dismutase is sufficient to induce amyotrophic lateral sclerosis in transgenic mice. *J Neurosci* 28:2075–2088.
7. Clement AM, *et al.* (2003) Wild-type nonneuronal cells extend survival of SOD1 mutant motor neurons in ALS mice. *Science* 302:113–117.
8. Beers DR, *et al.* (2006) Wild-type microglia extend survival in PU.1 knockout mice with familial amyotrophic lateral sclerosis. *Proc Natl Acad Sci USA* 103:16021–16026.
9. Boillee S, *et al.* (2006) Onset and progression in inherited ALS determined by motor neurons and microglia. *Science* 312:1389–1392.
10. Yamanaka K, *et al.* (2008) Astrocytes as determinants of disease progression in inherited amyotrophic lateral sclerosis. *Nat Neurosci* 11:251–253.
11. Howland DS, *et al.* (2002) Focal loss of the glutamate transporter EAAT2 in a transgenic rat model of SOD1 mutant-mediated amyotrophic lateral sclerosis (ALS). *Proc Natl Acad Sci USA* 99:1604–1609.
12. Van Damme P, *et al.* (2007) Astrocytes regulate GluR2 expression in motor neurons and their vulnerability to excitotoxicity. *Proc Natl Acad Sci USA* 104:14825–14830.
13. Nagai M, *et al.* (2007) Astrocytes expressing ALS-linked mutated SOD1 release factors selectively toxic to motor neurons. *Nat Neurosci* 10:615–622.
14. Di Giorgio FP, *et al.* (2007) Non-cell autonomous effect of glia on motor neurons in an embryonic stem cell-based ALS model. *Nat Neurosci* 10:608–614.
15. Misawa H, *et al.* (2003) VAChT-Cre.Fast and VAChT-Cre.Slow: Postnatal expression of Cre recombinase in somatomotor neurons with different onset. *Genesis* 37:44–50.
16. Gong YH, *et al.* (2000) Restricted expression of G86R Cu/Zn superoxide dismutase in astrocytes results in astrocytosis but does not cause motoneuron degeneration. *J Neurosci* 20:660–665.
17. Wong PC, *et al.* (1995) An adverse property of a familial ALS-linked SOD1 mutation causes motor neuron disease characterized by vacuolar degeneration of mitochondria. *Neuron* 14:1105–1116.
18. Zhou Q, Anderson DJ (2002) The bHLH transcription factors OLIG2 and OLIG1 couple neuronal and glial subtype specification. *Cell* 109:61–73.
19. Lu QR, *et al.* (2002) Common developmental requirement for Olig function indicates a motor neuron/oligodendrocyte connection. *Cell* 109:75–86.
20. Takebayashi H, *et al.* (2002) The basic helix–loop–helix factor olig2 is essential for the development of motoneuron and oligodendrocyte lineages. *Curr Biol* 12:1157–1163.
21. Bruijn LI, *et al.* (1997) ALS-linked SOD1 mutant G85R mediates damage to astrocytes and promotes rapidly progressive disease with SOD1-containing inclusions. *Neuron* 18:327–338.
22. Lobsiger CS, Garcia ML, Ward CM, Cleveland DW (2005) Altered axonal architecture by removal of the heavily phosphorylated neurofilament tail domains strongly slows superoxide dismutase 1 mutant-mediated ALS. *Proc Natl Acad Sci USA* 102:10351–10356.
23. Yamanaka K, *et al.* (2006) Progressive spinal axonal degeneration and slowness in ALS2-deficient mice. *Ann Neurol* 60:95–104.
24. Kong J, Xu Z (1999) Peripheral axotomy slows motoneuron degeneration in a transgenic mouse line expressing mutant SOD1 G93A. *J Comp Neurol* 412:373–380.
25. Miller TM, *et al.* (2006) Gene transfer demonstrates that muscle is not a primary target for non-cell-autonomous toxicity in familial amyotrophic lateral sclerosis. *Proc Natl Acad Sci USA* 103:19546–19551.
26. Zhong, Z. *et al.* (2008) ALS-causing SOD1 mutants generate blood-spinal cord barrier breakdown and reductions in microcirculation prior to motor neuron degeneration. *Nat Neurosci* 11:420–422.
27. Williamson TL, Cleveland DW (1999) Slowing of axonal transport is a very early event in the toxicity of ALS-linked SOD1 mutants to motor neurons. *Nat Neurosci* 2:50–56.
28. Kaspar BK, *et al.* (2003) Retrograde viral delivery of IGF-1 prolongs survival in a mouse ALS model. *Science* 301:839–842.
29. Pardo CA, *et al.* (1995) Superoxide dismutase is an abundant component in cell bodies, dendrites, and axons of motor neurons and in a subset of other neurons. *Proc Natl Acad Sci USA* 92:954–958.